J|A|C|S ARTICLES

Published on Web 03/12/2009

Helical Aromatic Oligoamide Foldamers as Organizational Scaffolds for Photoinduced Charge Transfer

Martin Wolffs,[†] Nicolas Delsuc,[‡] Dirk Veldman,[†] Nguyễn Vân Anh,[§] René M. Williams,[§] Stefan C. J. Meskers,[†] René A. J. Janssen,[†] Ivan Huc,*[,‡] and Albertus P. H. J. Schenning*[,†]

Laboratory of Macromolecular and Organic Chemistry, Eindhoven University of Technology, P.O. Box 513, 5600 MB Eindhoven, The Netherlands, Institut Européen de Chimie et Biologie, Université de Bordeaux, CNRS UMR5248, 2 rue Robert Escarpit, 33607 Pessac Cedex, France, and Molecular Photonics Group, Van't Hoff Institute for Molecular Sciences, University of Amsterdam, Nieuwe Achtergracht 166, 1018 WV Amsterdam, The Netherlands

Received December 1, 2008; E-mail: i.huc@iecb.u-bordeaux.fr; a.p.h.j.schenning@tue.nl

Abstract: Here we report the synthesis and characterization of four quinoline-derived foldamers with increasing oligomeric length; dimer **O2P**, tetramer **O4P**, pentamer **O5P**, and nonamer **O9P** functionalized with on one end an oligo(*p*-phenylene vinylene) (OPV) and on the other end a perylene bisimide (PB) chromophore. ^{1}H NMR confirms the formation of the expected folded structures in both toluene and chloroform solution. The structural predictability and rigidity of the oligomeric series enabled us to investigate the effect of a helical bridge and chromophore position on the photoinduced processes in the electron OPV−PB donor−acceptor pair in chloroform and toluene. The helical properties of the bridge ensured that the chromophore separation distance through space is different from the separation distance through the bridge. For all foldamer−solvent combinations studied, excitation of either OPV or PB results in nearly quantitative quenching of the fluorescence indicating a fast charge separation reaction between the OPV and PB. Femtosecond photoinduced absorption measurements confirmed the fast formation of a charge-separated state. The recombination reaction involves a combination of direct decay to the ground state and the formation of an intermediate triplet state, with their balance depending on the foldamer−solvent combination. Molecular orbital calculations rationalize the fast photoinduced charge separation, by revealing that the bridging foldamer mediates the charge transfer from donor to acceptor via the superexchange mechanism. Remarkably low attenuation factors ($\beta_{CS} \approx 10^{-2}$ Å^{-1}) were obtained using either through space or through bridge separation distance. However, in these calculations only three of the four foldamers show the expected linear behavior between the logarithm of the charge separation rate constant and the distance between the chromophores. The combined results show when a helical bridge is separating the charge transfer couple, hampering the usefulness of a uniform description of the charge-separation phenomena.

Introduction

Photoinduced charge-transfer processes are crucial for the function of the photosynthetic unit.[1,2] In particular, the spatial organization of the individual molecules within the photosynthetic unit imposed by the surrounding protein matrix enables the formation of a charge separated state with extraordinary long lifetimes.[1] In order to understand and mimic these biological photophysical processes, artificial model systems have been designed in which the distance dependence for charge separation and charge recombination reactions is studied in donor−bridge−acceptor molecules.[3,4] In these examples, the chromophores are either placed on top (cofacial) or next to each other (colinear). For instance a cofacial positioning of the chromophores is achieved by using helical DNA,[4] peptides,[2,5] aromatic foldamers,[6,7] or a nonhelical rigid linker[8] as a scaffold to attach the chromophores. Colinear interactions are obtained by connecting

[†] Eindhoven University of Technology.
[‡] Université de Bordeaux.
[§] University of Amsterdam.

(1) Hoeben, F. J. M.; Jonkheijm, P.; Meijer, E. W.; Schenning, A. P. H. J. *Chem. Rev.* **2005**, *105*, 1491–1546.
(2) (a) Giese, B. *Bioorgan. Med. Chem.* **2006**, *14*, 6139–6143. (b) *Charge Tranfser in DNA*; Wagenknecht, H.-A. Ed.; Wiley-VCH: Weinheim, Germany, 2005.
(3) (a) Paddon-Row, M. N. *Acc. Chem. Res.* **1994**, *27*, 18–25. (b) Benniston, A. C.; Harriman, A. *Chem. Soc. Rev.* **2006**, *35*, 169–179. (c) Verhoeven, J. W. *J. Photochem. Photobiol. C* **2006**, *7*, 40–60.
(4) (a) Fukui, K.; Tanaka, K *Angew. Chem., Int. Ed.* **1998**, *37*, 158–161. (b) Berlin, Y. A.; Burin, A. L.; Ratner, M. A. *Superlattices Microst.* **2000**, *28*, 241–252. (c) Giese, B. *Curr. Opin. Chem. Biol.* **2002**, *6*, 612–618. (d) Takada, T.; Kawai, K.; Tojo, S.; Majima, T. *Tetrahedron Lett.* **2003**, *44*, 3851–3854. (e) Lewis, F. D.; Zhang, L.; Zuo, X. *J. Am. Chem. Soc.* **2005**, *127*, 10002–10003. (f) Manetto, A.; Breeger, S.; Chatgilialoglu, C.; Carell, T. *Angew. Chem., Int. Ed.* **2006**, *45*, 318–321.
(5) Jones II, G.; Zhou, X.; Vullev, V. I. *Photochem. Photobiol. Sci.* **2003**, *2*, 1080–1087.
(6) Zeidan, T. A.; Wang, Q.; Fiebig, T.; Lewis, F. D. *J. Am. Chem. Soc.* **2007**, *129*, 9848–9849.
(7) Marcos Ramos, A.; Meskers, S. C. J.; Beckers, E. H. A.; Prince, R. B.; Brunsveld, L.; Janssen, R. A. J. *J. Am. Chem. Soc.* **2004**, *126*, 9630–9644.

the chromophores to rigid bridges that can either be composed of conjugated[3,9] or saturated moieties.[3,10] As a consequence of the rigidity of these bridges, in all cofacial and colinear positioning, the chromophore position is fixed and the distance between the chromophores through space is similar as the distance through the bridge. Depending on the properties of the bridge and the way the chromophores are attached to the bridge, charge transfer may proceed via a superexchange or a charge hopping mechanism.[11] In the superexchange mechanism the bridge solely serves to facilitate the interaction between the donor and acceptor wave functions. In the hopping mechanism the electron is located at the bridge for a short period of time during which the charge transfer occurs. The effectiveness of the bridge to mediate the charge transfer process is expressed in the attenuation factor β.[3,11] Typical attenuation factors found are $\beta = 0.6-1.2$ Å^{-1} for hydrocarbon bridges, $\beta = 0.32-0.66$ Å^{-1} for conjugated polyphenylenes, $\beta = 0.04-0.2$ Å^{-1} for polyenes and $\beta = 0.04-0.17$ Å^{-1} for polyynes.[12] A lower attenuation factor indicates that the bridges can more effectively mediate the charge transfer reaction.

The use of bridges to spatially organize chromophores in an intermediate situation where the chromophores are positioned in both a cofacial and a colinear arrangement has rarely been explored.[3b] Examples include the investigation of chromophores with constrained molecular assemblies[3b] or connected at ortho, meta, or para positions by rigid aromatic molecular linkers.[3b,8b−e,13] In both cases the chromophores are held at a relatively short distance from each other by nonhelical bridges. These studies revealed that the effect of chromophore orientation on the charge transfer process, if any, depends highly on the system at hand. One hurdle in studying the effect of chromophore positioning in both a cofacial and colinear arrangement lies in the difficulty to achieve large distances between the electron donor and acceptor and to simultaneously be able to control and tune their relative orientations. We devised that helical foldamers possessing stable and predictable conformations may be promising candidates, where the helicity of the bridge can be used as a scaffold to organize chromophores in space. Indeed, chemists have designed and synthesized a large variety of oligomeric and polymeric molecules that adopt predefined helical or extended conformations[14] that are commonly used as peptide mimics the sizes of which sometimes approach those of small proteins.[15]

Here, we report on the synthesis and characterization of a series of helical aromatic oligoquinoline amide-based foldamers acting as a helical bridge between an electron donor, an oligo(*p*-phenylene vinylene) (OPV) and an electron acceptor, a perylene bisimide (PB). We selected this charge transfer couple since the photophysics of the individual compounds and the charge-transfer pair have been thoroughly studied by us and others.[16,17] The oligoquinoline amide foldamers feature remarkably high structural robustness and predictability in a variety of apolar, polar, and protic solvents and in the solid state as determined with extensive NMR and single-crystal X-ray diffraction studies.[18] For example, the characteristic time of helix handedness inversion in chlorinated or aromatic solvents lies in the 100 ms range for a quinolinecarboxamide tetramer and in the 2 h range for an octamer.[18d] In DMSO, NMR experiments show that the helical structure of an octamer is stable up to 120 °C.[15a,18] These beneficial properties are expected to enable the exact positioning of the chromophores in order to vary and control not only the distance between the donor and the acceptor, but also their relative orientation in space. As a result of the helicity of the foldamers the distance between the chromophores either through space or through bridge is different. For this reason it is likely that the charge transfer pathways will depend on the foldamer

(8) (a) Wasielewski, M. R. *J. Org. Chem.* **2006**, *71*, 5051–5066. (b) Gouloumis, A.; González-Rodrigues, D.; Vázquez, P.; Torres, T.; Liu, S.; Echegoyen, L.; Ramey, J.; Hug, G. L.; Guldi, D. M. *J. Am. Chem. Soc.* **2006**, *128*, 12674–12684. (c) Hippius, C.; van Stokkum, I. H. M.; Gesänger, M.; Groeneveld, M. M.; Williams, R. M.; Würthner, F. *J. Phys. Chem. C.* **2008**, *112*, 2476–2486. (d) Hippius, C.; Schlosser, F.; Vysotsky, M. O.; Böhmer, V.; Würthner, F. *J. Am. Chem. Soc.* **2006**, *128*, 3870–3871. (e) Hippius, C.; van Stokkum, I. H. M.; Zangrando, E.; Williams, R. M.; Wykes, M.; Beljonne, D.; Würthner, F. *J. Phys. Chem. C* **2008**, *112*, 14626–14638.

(9) For example:(a) Wiberg, J.; Guo, L.; Pettersson, K.; Nilsson, D.; Ljungdahl, T.; Mårtensson, J.; Albinsson, B. *J. Am. Chem. Soc.* **2007**, *129*, 155–163. (b) Oike, T.; Kurata, T.; Takimiya, K.; Otsubo, T.; Aso, Y.; Zhang, H.; Araki, Y.; Ito, O. *J. Am. Chem. Soc.* **2005**, *127*, 15372–15373. (c) Vail, S. A.; Krawczuk, P. J.; Guldi, D. M.; Palkar, A.; Echegoyen, L.; Tomé, J. P. C.; Fazio, M. A.; Schuster, D. I. *Chem. Eur. J.* **2005**, *11*, 3375–3388. (d) Benniston, A. C.; Harriman, A.; Li, P.; Patel, P. V.; Sams, C. A. *Chem. Eur. J.* **2008**, *14*, 1710–1717.

(10) (a) Chen, K.-Y.; Hsieh, C.-C.; Cheng, Y.-M.; Lai, C.-H.; Chou, P.-T.; Chow, T. J. *J. Phys. Chem. A* **2006**, *110*, 12136–12144. (b) Williams, R. M.; Koeberg, M.; Lawson, J. M.; An, Y.-Z.; Rubin, Y.; Paddon-Row, M. N.; Verhoeven, J. W. *J. Org. Chem.* **1996**, *61*, 5055–5062.

(11) Lewis, F. D.; Zhu, H.; Daublain, P.; Fiebig, T.; Raytchev, M.; Wang, Q.; Shafirovich, V. *J. Am. Chem. Soc.* **2006**, *128*, 791–800.

(12) Ikemoto, I.; Takimiya, K.; Aso, Y.; Otsubo, T.; Fujitsuka, M.; Ito, O. *Org. Lett.* **2002**, *4*, 309–311.

(13) Thompson, A. L.; Ahn, T. S.; Thomas, K. R. J.; Thayumanavan, S.; Martínez, T. J.; Bardeen, C. J. *J. Am. Chem. Soc.* **2005**, *127*, 16348–16349.

(14) For reviews, see:(a) *Foldamers: Structure, Properties and Applications*; Hecht, S., Huc, I., Eds.; Wiley-VCH: Weinheim, Germany, 2007; (b) Goodman, C. M.; Choi, S.; Shandler, S.; DeGrado, W. F. *Nat. Chem. Biol.* **2007**, *3*, 252–262. (c) Hill, D. J.; Mio, M. J.; Prince, R. B.; Hughes, T. S.; Moore, J. S. *Chem. Rev.* **2001**, *101*, 3893–4011. (d) Li, Z.-T.; Hou, J.-L.; Li, C.; Yi, H.-P. *Chem. Asian J.* **2006**, *1*, 766–778. (e) Huc, I. *Eur. J. Org. Chem.* **2004**, 17–29. (f) Gong, B. *Chem. Eur. J.* **2001**, *7*, 4336–4342.

(15) (a) Delsuc, N.; Léger, J.-M.; Massip, S.; Huc, I. *Angew. Chem., Int. Ed.* **2007**, *46*, 214–217. (b) Daniels, D. S.; Petersson, E. J.; Qiu, J. X.; Schepartz, A. *J. Am. Chem. Soc.* **2007**, *129*, 1532–1534. (c) Horne, W. S.; Price, J. L.; Keck, J. L.; Gellman, S. H. *J. Am. Chem. Soc.* **2007**, *129*, 4178–4180. (d) Dolain, C.; Léger, J.-M.; Delsuc, N.; Gornitzka, H.; Huc, I. *Proc. Natl. Acad. Sci. U.S.A.* **2005**, *102*, 16146–16151.

(16) (a) Beckers, E. H. A.; Meskers, S. C. J.; Schenning, A. P. H. J.; Chen, Z.; Würthner, F.; Janssen, R. A. J. *J. Phys. Chem. A.* **2004**, *108*, 6933–6937. (b) Würthner, F.; Chen, C.; Hoeben, F. J. M.; Osswald, P; You, C.-C.; Jonkheijm, P.; van Herrikhuijzen, J.; Schenning, A. P. H. J.; van der Schoot, P. P. A. M.; Meijer, E. W.; Beckers, E. H. A.; Meskers, S. C. J.; Janssen, R. A. J. *J. Am. Chem. Soc.* **2004**, *126*, 10611–10618. (c) Beckers, E. H. A.; Jonkheijm, P.; Schenning, A. P. H. J.; Meskers, S. C. J.; Janssen, R. A. J. *ChemPhysChem* **2005**, *6*, 2029–2031. (d) Beckers, E. H. A.; Meskers, S. C. J.; Schenning, A. P. H. J.; Chen, Z.; Würhtner, F.; Janssen, R. A. J. *J. Am. Chem. Soc.* **2006**, *128*, 649–657. (e) Beckers, E. H. A.; Meskers, S. C. J.; Jonkheijm, P.; Schenning, A. P. H. J.; Chen, Z.; Würthner, F.; Janssen, R. A. J. *J. Phys. Chem. B* **2006**, *110*, 16967–16978. (f) Jonkheijm, P.; Stutzmann, N.; Chen, C.; de Leeuw, D. M.; Meijer, E. W.; Schenning, A. P. H. J.; Würthner, F. *J. Am. Chem. Soc.* **2006**, *128*, 9535–9540.

(17) Examples concerning perylene bisimide studies:(a) Baffreau, J.; Leroy-Lhez, S.; Hudhomme, P.; Groeneveld, M. M.; van Stokkum, I. H. M.; Williams, R. M. *J. Phys. Chem. A* **2006**, *110*, 13123–13125. (b) Pagès, S.; Langm, B.; Vauthey, E. *J. Phys. Chem. A* **2006**, *110*, 7547–7533. (c) Fron, E.; Bell, T. D. M.; Van Vooren, A.; Schweitzer, G.; Cornil, J.; Beljonne, D.; Toele, P.; Jacob, J.; Müllen, K.; Hofkens, J.; Van der Auweraer, M.; De Schryver, F. C. *J. Am. Chem. Soc.* **2007**, *129*, 610–619. (d) Flamigni, L.; Ventura, B.; Tasior, M.; Becherer, T.; Langhals, H.; Gryko, T. G. *Chem. Eur. J.* **2008**, *14*, 169–183.

(18) (a) Jiang, H.; Léger, J.-M.; Huc, I. *J. Am. Chem. Soc.* **2003**, *125*, 3448–3449. (b) Dolain, C.; Grélard, A.; Laguerre, M.; Jiang, H.; Maurizot, V.; Huc, I. *Chem. Eur. J.* **2005**, *11*, 6135–6144. (c) Gillies, E. R.; Dolain, C.; Léger, J.-M.; Huc, I. *J. Org. Chem.* **2006**, *71*, 7931–7939. (d) Delsuc, N.; Kawanami, T.; Lefeuvre, J.; Shundo, A.; Ihara, H.; Takafuji, M.; Huc, I. *ChemPhysChem* **2008**, *9*, 1882–1890.

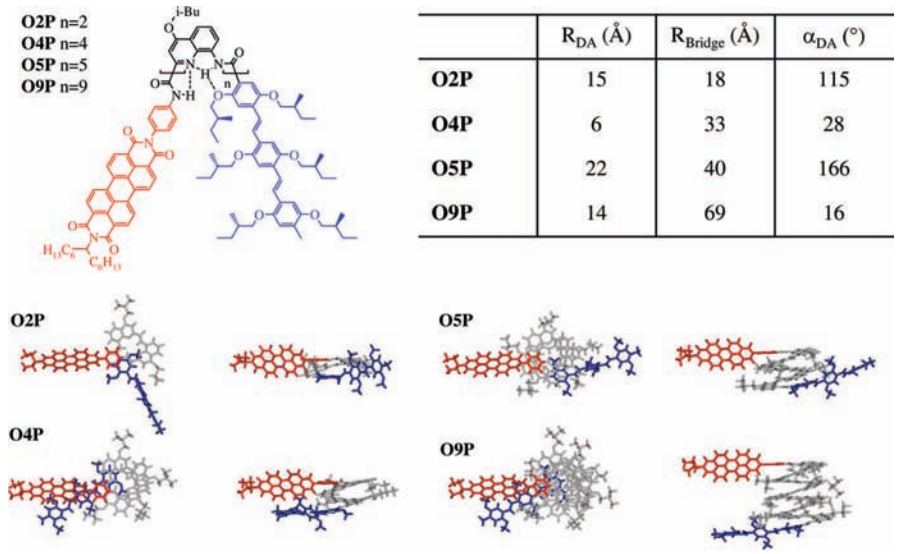

	R_{DA} (Å)	R_{Bridge} (Å)	α_{DA} (°)
O2P	15	18	115
O4P	6	33	28
O5P	22	40	166
O9P	14	69	16

Figure 1. Molecular formula of the four foldamers with appended chromophores (top left) described in this study. Table with the distance through space (R_{DA}) or through bridge (R_{Bridge}) and dihedral angle (α_{DA}) between the chromophores (top right), and top views down the foldamer helix axis (left) and side views (right) of their energy minimized conformations (bottom). The helix backbones are shown in gray, the OPV units in blue, and the PB units in red. The alkyl chains of OPV and PB units were replaced by methyl groups during energy minimization. The top views clearly show the similar orientations of the chromophores in **O4P** and **O9P**.

that is studied. We synthesized four different foldamers sequences ranging from dimer to nonamer that are all equipped with the same electron donor (OPV) and electron acceptor (PB) rigidly connected to the quinoline foldamer (Figure 1). These molecules were designed to cover a well-defined array of distances and orientations between the chromophores. With a variety of optical techniques we show that excitation of the PB leads to the formation of a charge separated state. Remarkable low attenuation factors are obtained by either using the distance through space ($\beta_{CS} = 0.05$ Å^{-1}) or through the bridge ($\beta_{CS} = 0.02$ or 0.06 Å^{-1}). Molecular orbital calculations revealed electronic coupling through the bridging foldamer, where the degree of electronic interaction depends highly on the foldamer studied. These results show that the bridge is most likely mediating the charge separation between the chromophores. However, the calculations performed to ascertain the attenuation factor is each time based on only three foldamers while a fourth one deviates. The current theoretical description that dictates an exponential relationship between the charge-transfer rates and the distance between the donor and acceptor, being either the distance through space or through a bridge, seems to be insufficient to uniformly describe the charge separation phenomena when a helical bridge is separating the charge transfer couple.

Results and Discussion

Molecular Design. The calculation of the energy-minimized structures of all oligomers from dimer to nonamer by molecular mechanics enabled us to select a series of foldamers where both the orientation and the distance could be varied.[19] To minimize the complexity of the calculations, the aliphatic tails of the chromophores were shortened. In order to reduce the synthetic effort, we decided to select four different foldamers for this study. The analyses of the optimized structures revealed that the four foldamers listed in Figure 1 cover a wide variety of orientations and distances between the chromophores, and were for that reason synthesized. In **O2P** the center-to-center donor−acceptor distance through space (R_{DA}) between the chromophores is calculated to be 15 Å and the angle between them is $\alpha_{DA} = 115°$. The separation through the bridge (R_{Bridge}) is calculated as the shortest distance across the quinoline units, resulting in $R_{Bridge} = 18$ Å for **O2P**. The tetramer **O4P** ($R_{Bridge} = 33$ Å) and nonamer **O9P** ($R_{Bridge} = 69$ Å) both place the donor under a small angle with respect to the acceptor ($\alpha_{DA} = 28°$ for **O4P** and $\alpha_{DA} = 16°$ for **O9P**) separated by 6 and 14 Å, respectively, which can suggest that the charge separation pathways can be similar for these two compounds. The structures of **O2P** and **O9P** show that the distance through space between the chromophores is similar in the 2-foldamers, while the distance through the bridge (18 vs 69 Å) differs considerably. Therefore, a comparison between the results for these two foldamers should yield more insight in the effect of chromophore orientation and charge separation pathway. In the pentamer **O5P** a shorter through bridge separation distance than in **O9P** is achieved (40 vs 69 Å), while the through-space distance between the chromophores is increased to 22 Å since the chromophores are almost radially opposed ($\alpha_{DA} = 166°$).[20]

Synthesis and Characterization. The synthesis of **O2P**, **O4P**, **O5P**, and **O9P** starts from the previously reported, perylene bisimide **1**,[21] OPV **2**,[22] and quinoline derivatives.[23]

The synthesis of **O2P** starts with a peptide-based HBTU-activated coupling of **1** with nitro quinoline dimer carboxylic acid **5** resulting in **6** with 60% yield after column chromatography. Catalytic hydrogenation in chloroform with 10% Pd on carbon converts the nitro derivative **6** to amine **7** in quantitative yield. Subsequent acylation of **7** with **2** and purification by

(19) Mohamadi, F.; Richards, N. G. J.; Guida, W.-C.; Liskamp, R.; Lipton, M.; Caufield, C.; Chang, G.; Hendrickson, T.; Still, W. C. *J. Comput. Chem.* **1990**, *11*, 440–467.

(20) The OPV moiety bears an intrinsic chirality in the methylbutoxy side chains for an attempt to bias the helical handedness of the foldamer to either a right-handed (P) helix or a left-handed (M) helix, as observed previously for these foldamers.[26]

(21) Yan, P.; Holman, M. W.; Robustelli, P.; Chowdhury, A.; Ishak, F. I.; Adams, D. M. *J. Phys. Chem. B* **2005**, *109*, 130–137.

(22) Schenning, A. P. H. J.; Peeters, E.; Meijer, E. W. *J. Am. Chem. Soc.* **2000**, *122*, 4489–4495.

recycling gel permeation chromatography (GPC) eventually yields 17 mg (30%) of **O2P** as an orange solid. Although this synthetic route is in principle generally applicable to synthesize all foldamers, we found that in practice, the hydrogenation conditions caused the degradation of the perylene-nitro-tetramer. By using protective group chemistry as depicted in Scheme 1, this troublesome hydrogenation could be circumvented. To this end, the tetramer amine-ester was protected with a BOC group by treatment with di-*tert*-butyl dicarbonate that resulted in the protected amine **9**. Subsequent hydrolysis of the methyl ester of **9** and activation of the corresponding carboxylic acid **10** to acid chloride **11** under mild conditions by using a chloroenamine was followed by a reaction with PB amine **1** resulting in **12** after column chromatography. Removal of the BOC group with trifluoroacetic acid in dichloromethane yielded **13** quantitatively and subsequent coupling with **2** under basic conditions resulted in tetramer **O4P** as an orange solid after purification by column chromatography and recycling GPC.

For the synthesis of **O5P** and **O9P** a more convergent synthetic strategy (Scheme 1) was applied which is based on the chain extension of a foldamer with one monomeric unit that already contains the OPV chromophore. Although this synthetic scheme seems applicable for the synthesis of all the foldamers, it is hampered by the synthetic availability of the starting compounds. The synthetic strategy used to synthesize the starting foldamers is based on connecting even numbers of oligomers making dimer, tetramer (**3**), and octamer (**4**) readily available.[14e,23] The synthesis of the monomeric building blocks starts with an acid chloride coupling of **2** with amine **14** (70%). Subsequent hydrolysis of the ester and activation with a chloroenamine ultimately yielded monomeric building block **17**. This compound can be attached to either the tetramer (**3**) or octamer (**4**) amine. Chain extension of **3** and **4** with one monomeric unit **17** resulted in pentamer **18** and nonamer **19**, respectively. The esters were hydrolyzed to their corresponding acids (for pentamer compound **20** and for nonamer compound **21**) with sodium hydroxide in a THF/methanol mixture and the carboxylic acids were activated with a chloroenamine to the acid chlorides **22** and **23**. PB amine **1** was coupled to the acid chlorides which resulted in pentamer **O5P** and nonamer **O9P** that were intensively purified by recycling GPC. All intermediate compounds have been analyzed with ^{1}H NMR and/or MALDI-TOF MS, while additional GPC and ^{13}C NMR measurements were performed for the final products.[24,25]

As shown by the ^{1}H NMR spectra in Figure 2, the amide protons involved in intramolecular hydrogen bonds are shifted downfield and appear as sharp signals, as expected for folded oligoquinolines.[18] Upon increasing the oligomer length, these protons shift upfield, indicating an increase of ring current effects associated with aromatic stacking in the helical structure. A similar trend is observed for the aromatic signals. For example, a signal assigned to an OPV resonance is found at $\delta = 6.2$ ppm in **O2P** and **O4P**, at $\delta = 6.1$ ppm in **O5P**, and at $\delta = 5.8$ ppm in **O9P**.[25] In toluene-d_8, the shielding effect seems to be more important for the amide protons resulting in a larger upfield shift. An important observation is the splitting of a number of signals of **O4P**, **O5P**, and **O9P** in $CDCl_3$ and toluene-d_8, revealing the presence of two diastereomers in solution with a 1:1 ratio of P and M helices.[18] The result is in contrast with previous reports about quinoline amide foldamers appended with chiral residues, which did show a preference for the helical handedness.[20,26] The stereocenters carried by the OPV are located further away from the helix which most likely hampers any significant interactions with the helical backbone that would favor one particular handedness. The exchange between the P helix and the M helix is slow on the NMR time scale (milliseconds), and thus, the two species appear as two sets of signals.[26] Only for the shorter oligomer **O2P**, the exchange is fast and the average NMR signals of the diastereomers are observed. The lack of preference in helical handedness is confirmed by the circular dichroism spectra that are essentially nonexistent (not shown). Since the helical diastereoisomers only differ by the P or M helical sense of the quinoline oligomer, the position of the chromophores with respect to the helix and with respect to each other is expected to remain the same in the P and M helices which, for the purpose of this study, may be considered as enantiomers. This assumption is validated by molecular modeling, which shows no change of the conformation when the stereochemistry of the OPV is inverted while the handedness of the helix is conserved.[27]

UV/Vis Absorption. To study the effect of solvent polarity on the charge-transfer processes, the photophysical studies were performed in toluene and chloroform, since the structure of the quinoline foldamers is well established in both solvents.[18] The UV/vis absorption spectrum of each foldamer is shown in Figure 3 and can roughly be divided into three regions: a quinoline part (300−400 nm), an OPV part (350−450 nm), and a PB part (450−550 nm), as observed from the spectra of the individual chromophores in chloroform (Figure 3C). The quinoline part shows a progressive increase in molar absorption coefficient upon elongation as a result of the increase in quinoline content. The OPV and PB part only show small fluctuations in molar absorption coefficient that are likely caused by changes in electronic structure and environment, as also observed by ^{1}H NMR.[25] The difference between the absorption spectra of **O4P** when compared with the sum spectrum of the reference compounds indicates the existence of some electronic interaction in the ground state. The structure and spectral position of the vibronic bands of the PB are similar for all foldamers and are indicative for a molecularly dissolved chromophore. Even at high concentration ($c = 5.0 \times 10^{-4}$ M) the spectrum displays this characteristic vibronic progression and therefore ensures that further photophysical analysis is not hampered by any aggregation phenomena.[25] Decreasing the solvent polarity by using toluene instead of chloroform did not affect the shape of the absorption spectra or the position of the absorption maxima of the foldamers. Irrespective of the concentration, **O5P** and **O9P** show an overall decrease in molar absorption coefficient in toluene when compared to chloroform. Again the change in molar absorption coefficient is likely related to the differences in electronic structure and environment of the foldamers in the two solvents as also observed by ^{1}H NMR. Tabulated values of the molar absorption coefficients for the three regions are listed in the Supporting Information.

Fluorescence Spectroscopy. In order to evaluate the photophysical processes in these systems, steady-state emission spectra of the foldamers were recorded after excitation of either

(23) Jiang, H.; Léger, J.-M.; Dolain, C.; Guionneau, P.; Huc, I. *Tetrahedron* **2003**, *59*, 8365–8374.
(24) There was not enough material of **O5P** and **O9P** to obtain a good ^{13}C NMR after recycling GPC.
(25) See Supporting Information.
(26) Dolain, C.; Jiang, H.; Léger, J.-M.; Guionneau, P.; Huc, I. *J. Am. Chem. Soc.* **2005**, *127*, 12943–12951. (a) Jiang, H.; Dolain, C.; Léger, J.-M.; Gornitzka, H.; Huc, I. *J. Am. Chem. Soc.* **2004**, *126*, 1034–1035.
(27) These data are not reported here.

Scheme 1. Chromophoric Precursor Perylene Bisimide Amine **1**, OPV3-Acid Chloride **2**, Quinoline Tetramer **3**, and Octamer **4** Nitro Esters and the Synthetic Scheme of **O2P**, **O4P**, **O5P**, and **O9P**[a]

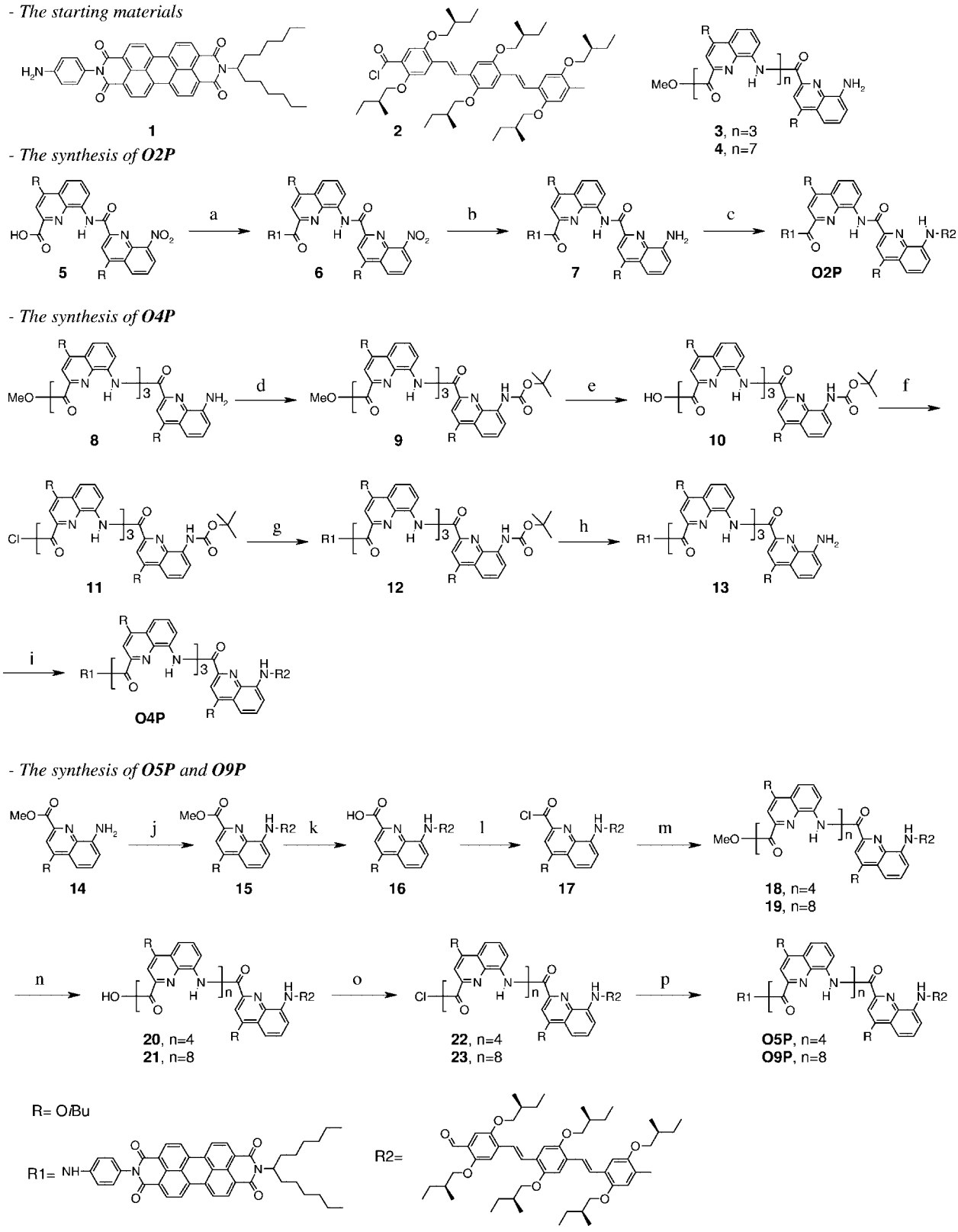

[a] (a) *o*-(Benzotriazol-1-yl)-*N*,*N*,*N*′,*N*′-tetramethyluronium hexafluorophosphate (HBTU), 1-hydroxybenzotriazole (HOBt), *N*,*N*-diisopropylethylamine (DIPEA), dimethylformamide (DMF), chloroform ($CHCl_3$), **1**, 24 h, RT, 60%; (b) H_2, 10% Pd/C, $CHCl_3$, 20 h, RT, 99%; (c) **2**, DIPEA, dry $CHCl_3$, 17 h, RT, 30%; (d) di-*tert*-butyl carbonate, 4-dimethylaminopyridine, 16 h, 40 °C, 76%; (e) sodium hydroxide, tetrahydrofuran (THF)/methanol (10: 1 v/v), 16 h, 40 °C, 62%; (f) 1-chloro-*N*,*N*-2-trimethylpropenylamine, dry CH_2Cl_2, 17 h, RT, 99%; (g) **1**, DIPEA, dichloromethane (CH_2Cl_2) /THF (1:1 v/v) 16 h, RT, 68%; (h) trifluoracetic acid/CH_2Cl_2 (1:1 v/v), 3 h, RT, 99%; (i) **2**, DIPEA, 20 h, RT, 17%; (j) **2**, DIPEA, CH_2Cl_2, 4 h, 70%; (k) sodium hydroxide, THF/methanol (10:1 v/v), 40 °C, 20 h, 95%; (l) 1-chloro-*N*,*N*-2-trimethylpropenylamine, dry CH_2Cl_2, 17 h, RT, 99%; (m) DIPEA, CH_2Cl_2, 16 h, RT, Pentamer: **3**, 61%, Nonamer: **4**, 56%; (n) sodium hydroxide, THF/methanol (10:1 v/v), 40 °C, 20 h, Pentamer: 95%, Nonamer: 50%; (o) 1-chloro-*N*,*N*-2-trimethylpropenylamine, dry CH_2Cl_2, 17 h, RT, 99% for both; (p) DIPEA, THF/CH_2Cl_2 (2:1 v/v), 16 h, RT, 17% for both.

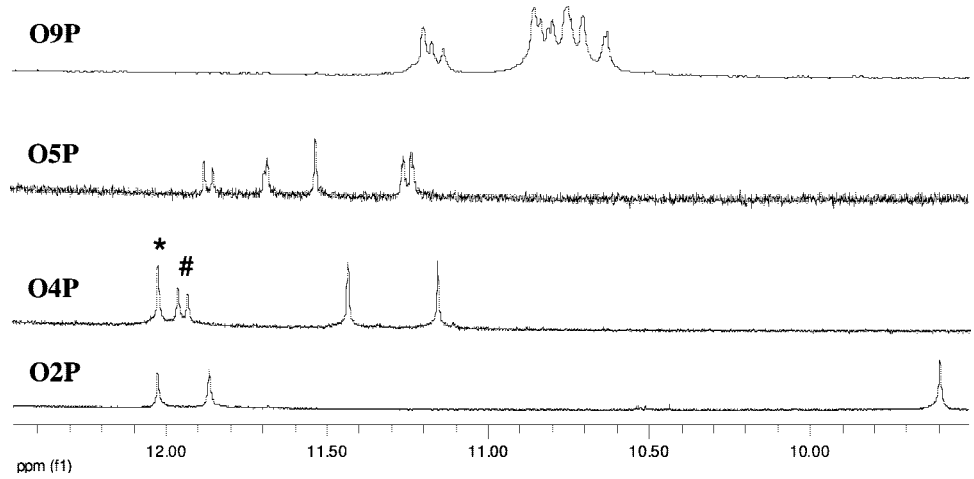

Figure 2. ^{1}H NMR spectra of the amide region for the four different foldamers in $CDCl_3$. One of the four amide resonances of **O4P** splits into two (as marked by * and #) corresponding to helical diastereomers. The same occurs to four of the five amide resonances of **O5P** and several resonances of **O9P**.

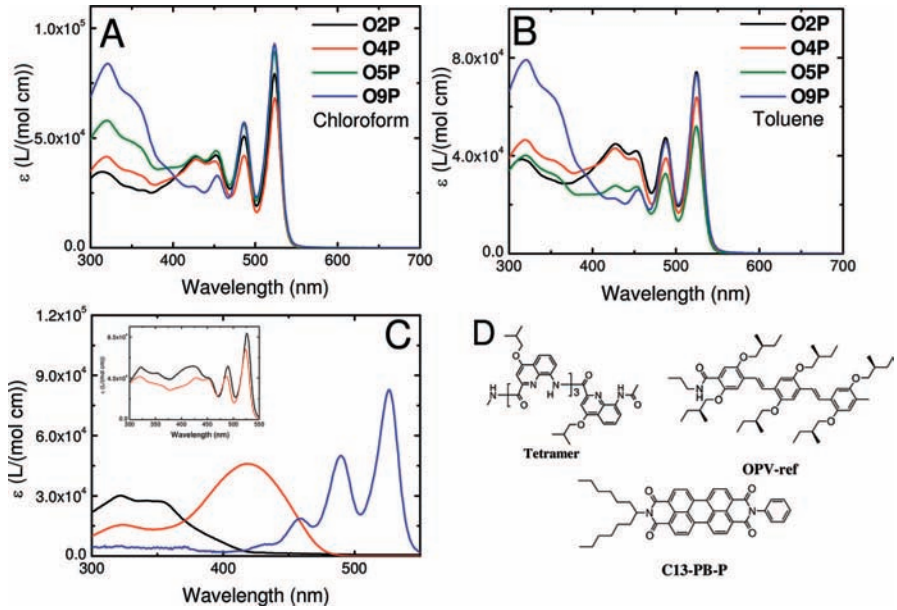

Figure 3. UV/vis absorption spectra of **O2P** (black), **O4P** (red), **O5P** (green), and **O9P** (blue) in chloroform (A) and toluene (B). The spectra of **Tetramer** (black), **OPV-ref**[22] (red), and **C13-PB-P**[25](blue) references in chloroform (C) and their molecular structures (D). The inset in C shows the sum-spectrum of the references (black) and of **O4P** (red).

the PB (495 nm) or the OPV (400 nm) chromophore.[25] Irrespective of excitation wavelength and solvent, the quantum yields of fluorescence for the PB are strongly diminished (Table 1). Although **C13-PB-P** does not have an amide functionality at the para position of the phenyl group, previous results of a compound having an urea functionality showed similar photophysical properties as **C13-PB-P**.[28] This indicates a highly efficient charge transfer reaction between the OPV and the PB.[16,29] Excitation spectra recorded at the residual emission band of the PB (577 nm) show contributions of all chromophores,[25]revealing that both the quinoline foldamer and the OPV chromophore contribute to an energy transfer reaction to the PB.

Table 1. Fluorescence Quantum Yields and Decay Times from Steady State and Time-Resolved Fluorescence, and Quenching Factors Derived Thereof

	chloroform				toluene			
	Φ_f (%)[a]	Q^a	τ (ps)[b]	Q^b	Φ_f (%)[a]	Q^a	τ (ps)[b]	Q^b
O2P	<1	>100	<50	>85	1.5	65	<50	>85
O4P	<1	>100	<50	>85	<1	>100	55	75
O5P	<1	>100	<50	>85	1.5	65	85	50
O9P	<1	>100	<50	>85	1.7	60	120	35

[a] Fluorescence quantum yield (Φ_f) and quenching factor (Q) from steady-state fluorescence using **C13-PB-P** as a reference (Φ_f(**C13-PB-P**) = 0.99), λ_{exc} = 495 nm.[25,30] [b] Emissive decay time (τ) and quenching factor (Q) from time-resolved fluorescence measurements using **C13-PB-P** as a reference (τ(**C13-PB-P**) = 4.2 ns).[25,30]

(28) Neuteboom, E. E.; Beckers, E. H. A.; Meskers, S. C. J.; Meijer, E. W.; Janssen, R. A. J. *Org. Biomol. Chem.* **2003**, *1*, 198–203.
(29) Cyclic voltammogram measurements performed on **Tetramer** (Figure 3D) did not yield any oxidation or reduction waves. This makes it very unlikely that the foldamer will participate in an electron-transfer reaction, even though, in principle, redox potential may differ in the excited state, see Supporting Information.

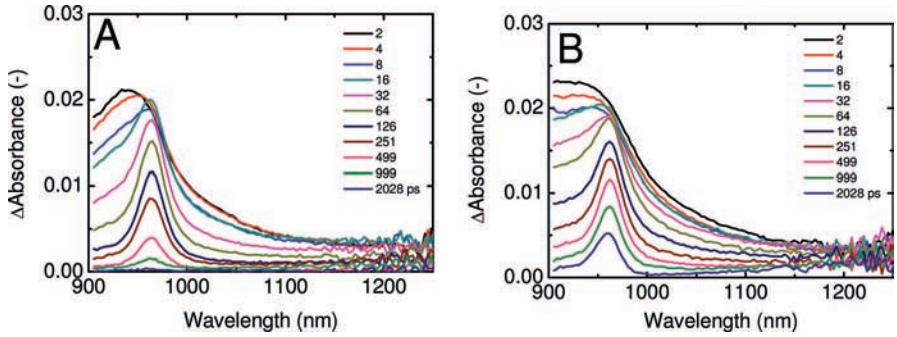

Figure 4. Femtosecond photoinduced absorption measurements of **O4P** in chloroform (A) and **O5P** in toluene (B) (optical density (OD) = 0.5 at λ_{exc} = 525 nm in a 2 mm quartz cell).

Time-resolved fluorescence spectroscopy showed significant quenching of the singlet excited state of the PB (577 nm) after excitation at $\lambda_{ex} = 400$ nm. Analysis of the decay traces resolved rise times (positive amplitude) that are shorter than the instrument response (30 ps) and short decay times (Table 1) close to the instrument response.[25] The rise times are attributed to energy transfer from OPV to PB, while the decay times result from the charge-transfer step. Although the low fluorescence intensity and very short decay times hinder accurate determination of the quenching factors, the results obtained from these decay times show reasonable correlation with the values from steady-state fluorescence. Photoinduced absorption spectroscopy will provide a more direct route to probe the charge transfer rates.

Photoinduced Absorption Spectroscopy. In order to elucidate if charge transfer is responsible for the observed fluorescence quenching, femtosecond photoinduced absorption spectroscopy was employed. With this technique, the rate of charge separation and charge recombination can be measured. Two representative transients, **O4P** in chloroform and **O5P** in toluene, are shown in Figure 4.

After excitation of the solution at $\lambda_{exc} = 525$ nm (PB chromophore), the transient absorption measurements in the near-infrared regime initially show a broadband (900−1100 nm) that sharpens in time into a band with a maximum at 961 nm. Reference experiments showed that the broadband relates to the S_1-S_n absorption of the PB,[25] while the absorption at 961 nm has been previously assigned to the absorption of the radical anion.[31] In addition the radical cation of the OPV trimer ($\lambda_{max} = 1630$ and 725 nm)[32] and the quinoline radical anion ($\lambda_{max} \approx 710$ nm)[33] and cation ($\lambda_{max} = 620$ nm)[34] do not absorb in the measured wavelength regime. Both bands are observed in all transient absorption spectra of the different foldamers, irrespective of the solvent used.[25] This indicates that in all systems excitation of the PB results in a charge separated state where the OPV acts as the electron donor and the PB as acceptor. The absence of signatures characteristic for the quinoline in the photoinduced measurements and the fact that the quinolines are not able to be oxidized or reduced by the chromophores strongly suggest that charge transfer between OPV and PB occurs via the superexchange mechanism.[11,16,29] The time constants of charge separation (τ_{CS}) and recombination (τ_{CR}) have been extracted from the traces at two different wavelengths. The traces at both wavelengths were simultaneously fitted with three different time constants, τ_{CS}, τ_{CR}, and a time constant of ~2 ps to account for solvent reorganization, including the restriction that all three time constants should yield the same result for both traces. For details about the fitting procedure, we refer the reader to the Supporting Information. The results of the fits are summarized in Table 2. Since no additional time constants were necessary for the fit, we assume that the two diastereoisomers present in a 1:1 ratio show virtually identical photophysics and behave as enantiomers, as expected from molecular mechanics calculations which revealed similar structural features for the diastereoisomers.

Table 2. Time Constants for Charge Separation (CS) and Charge Recombination (CR) in Chloroform and Toluene for **O2P**, **O4P**, **O5P**, and **O9P** from Femtosecond Photoinduced Absorption Measurements

	chloroform		toluene	
foldamer	τ_{CS} (ps)	τ_{CR} (ps)	τ_{CS} (ps)	τ_{CR} (ps)
O2P	20	240	20	1150
O4P	35	320	30	400
O5P	70	2140	110	1060
O9P	50	740	90	460

From Table 2 it is clear that charge separation is always faster than charge recombination. The short time constants for charge separation indicate that the formation of the charge separated state is much faster than the intrinsic decay of the PB acceptor-reference chromophore (**C13-PB-P**, Figure 3D).[25] This compound has a fluorescence quantum yield of near unity and its decay to the ground state proceeds in 4.2 ns.[30] Therefore, the observed low-fluorescence quantum yields in the order of 1% for these systems are in line with the 100-fold reduction of the decay rate (40 ps vs 4.2 ns). As expected and in correspondence to the fluorescence measurements, charge separation is at a similar rate or somewhat slower in toluene than in the more polar solvent chloroform, indicating that it occurs in the Marcus normal region.[35] There is no direct correlation between the through-bridge distance (R_{Bridge}) and charge-separation rates, confirming that the bridge is indeed folded. As expected for these folded structure, the rates do not follow the general trends normally observed for studies in which chromophores are oriented either in a cofacial or colinear fashion.[3−6] It is striking that the difference in charge separation lifetime between the two solvents is largest for the longer oligomers. When plotting the logarithm of the rate constants ($k = 1/\tau$) for charge separation

(30) Veldman, D.; Chopin, S. M. A.; Meskers, S. C. J.; Groeneveld, M. M.; Williams, R. M.; Janssen, R. A. J. *J. Phys. Chem. A* **2008**, *112*, 5846–5857.
(31) Salbeck, J. *J. Electroanal. Chem.* **1992**, *340*, 169–195.
(32) van Hal, P. A.; Beckers, E. H. A.; Peeters, E.; Apperloo, J. J.; Janssen, R. A. J. *Chem. Phys. Lett.* **2000**, 403–408.
(33) Hiratsuka, H.; Sekiguchi, K.; Hatano, Y.; Tanizaki, Y.; Mori, Y. *Can. J. Chem.* **1987**, *65*, 1185–1189.
(34) Kato, T.; Shida, T. *J. Am. Chem, Soc.* **1979**, *101*, 6869–6876.
(35) Marcus, R. A. *J. Chem. Phys.* **1965**, *43*, 679–701.

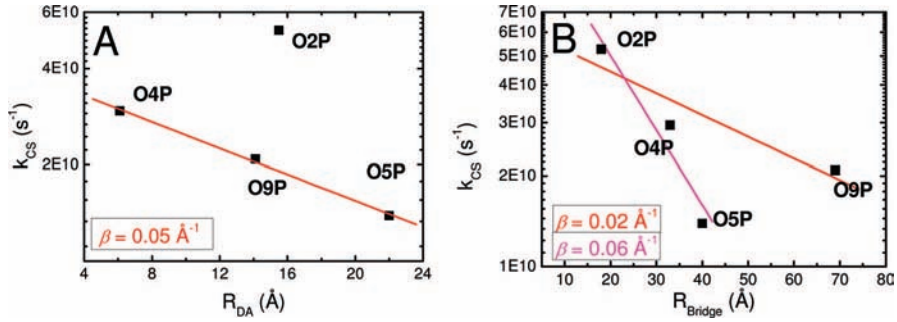

Figure 5. Dependence of the charge separation rate constant with the separation distance through space (A) or bridge (B). The red and purple values give the attenuation factors obtained directly from the linear fit (red, discarding **O5P**; purple, discarding **O9P** line).[25]

and charge recombination against the distance through space between the chromophores (R_{DA}), the three points belonging to **O4P**, **O5P**, and **O9P** are on a straight line while the shortest oligomer **O2P** deviates.[25,36] The slope of this line yields the attenuation factor $\beta_{CS} = 0.05$ Å^{-1} for charge separation in both solvents (Figure 5A) and $\beta_{CR} = 0.13$ Å^{-1} for charge recombination in chloroform (vide infra).[25] From the molecular structure it is clear that the helical bridge is not π-conjugated; however, the attenuation factor for charge separation is much lower than normally observed for charge separation through a conductive π-conjugated bridge (0.32−0.66 Å^{-1}) and is in the range of polyynes (0.04−0.17 Å^{-1}).[12] This surprisingly fast charge transport in the system indicates the presence of strong electronic interactions between the donor, acceptor, and bridge in the excited state and suggests a charge separation reaction that is mediated by the bridging foldamer.[3−6] For that reason we also plotted the logarithm of the charge-separation rate constant against the distance through the bridge (Figure 5B). From this plot it is clear that either **O5P** or **O9P** deviates from the straight line that is formed by the remaining molecules. The attenuation factor obtained in this way is again very low, $\beta_{CS} = 0.02$ Å^{-1} when discarding **O5P** and $\beta_{CS} = 0.06$ Å^{-1} when discarding **O9P** (Figure 5B), and remarkably similar when the through space chromophore separation is used. Although the attenuation factor seems to be independent of the distance that is used to calculate it, one should remember that for all three methods a different foldamer is discarded from the calculations. Therefore, a uniform theoretical description of the charge separation by using either the separation distance through space or through bridge is not possible when using helical bridges to separate the chromophores.

To shed more light on the low attenuation factor and the deviation of one of the foldamers with respect to the three others when calculating β, we performed AM1 calculations using SPARTAN (Wave function Inc.).[25] Within a frontier molecular orbital (FMO) description, excitation with, e.g., 530 nm corresponds to local PB excitation and in the acceptor-reference compound **C13-PB-P** this corresponds to the HOMO−LUMO transition.[25] The **O2P**, **O4P**, **O5P**, and **O9P** systems show analogous electronic transitions.[25] But, whereas the LUMO of these systems is very similar to the LUMO of the reference and entirely localized on the PB,[25] the highest occupied molecular orbital that has a contribution on the PB unit also has a significant, but varying, electron delocalization into the foldamer bridge (Figure 6). Of course, there are additional lower-lying doubly occupied orbitals that have a more pronounced PB contribution, but the delocalized orbitals depicted in Figure 6 will contribute to the "local PB excitation" and enhance the electronic coupling in the excited state between PB and OPV units. The HOMO-acceptor orbitals considered in Figure 6 serve to visualize how the π systems of the separate foldamer units mix into the large aromatic PB localized orbital resulting in electron delocalization of the PB orbital over the foldameric part in an oscillating mode. Within a FMO description, excitation of the PB is followed by charge separation which can be viewed as a HOMO acceptor−HOMO donor interaction.

The relevant HOMO-acceptor orbital of **O9P** is shown in Figure 6D (in fact, this is the HOMO-7 of the whole **O9P** system), the corresponding HOMO-donor orbital is shown in the Supporting Information (this is the HOMO orbital of the whole **O9P** system). It can be seen that this OPV-localized orbital also has substantial orbital coefficients on the foldamer bridge (just like the HOMO-7 of the system, but not as extensive) and the interaction of the HOMO and HOMO-7 strongly suggests electronic coupling through the foldamer bridge, and therefore, it is likely that the helical bridge mediates the charge transfer process. These calculations further support that charge separation through the bridge is achieved via the superexchange mechanism. In a similar way the charge recombination can be described by a LUMO-acceptor/HOMO-donor interaction.[25] The fact that the LUMO of all four foldamers is very similar and localized on the PB correlates with the much higher attenuation factor for charge recombination that is derived from the experiments.

The electronic coupling through the foldamer bridge as visualized by the MO calculations occurs to a different extent for all foldamers and is expected to slightly modulate the molar absorption coefficients of the different systems (see UV/vis in Figure 3). Because of the presence of only two bridge units in **O2P**, a significant amount of electronic coupling between the electron donor and acceptor exists which can account for the surprisingly fast charge separation reaction in this system (Figure 6A). This may explain the deviation of **O2P** from the other three oligomers when the distance through space is used to obtain the attenuation factor (Figure 5A). This enhanced electronic coupling also makes it difficult to compare **O2P** with **O9P** and with that to ascertain the effect of chromophore orientation on the charge transfer processes. From the MO calculations it becomes apparent that although the number of monomeric units is higher in the nonamer **O9P**, the electronic coupling is more pronounced than in **O5P**, where it is almost absent (Figure 6C vs D). For this reason it seems more likely that in **O9P** the charge separation is mediated by the bridging foldamer and that **O5P** is the molecule that deviates when the

(36) When the edge-to-edge distance was used, the attenuation factor was $\beta = 0.09$ Å^{-1} when discarding **O5P** from the fit.

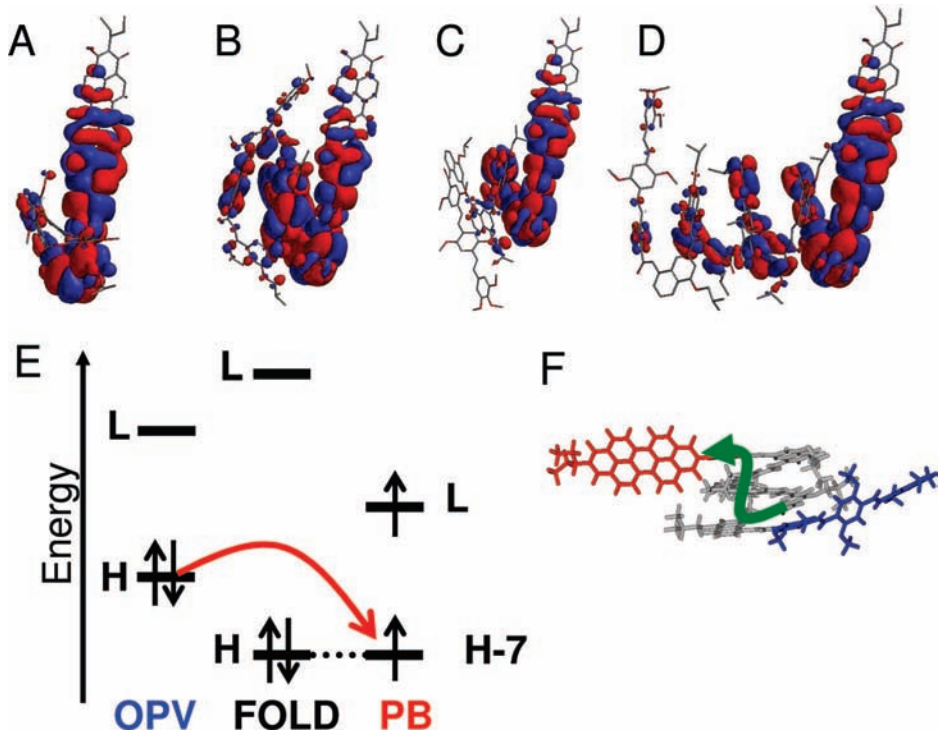

Figure 6. Visualization of the highest doubly occupied molecular orbitals of the foldamers with a contribution on the PB unit for **O2P** (A), **O4P** (B), **O5P** (C), and **O9P** (D). These orbitals contribute to the locally PB excited state and give evidence of coupling with the bridge. Schematic representation of the energy levels and the charge-transfer process between the OPV and PB in the **O9P** after excitation of the HOMO-7, where H stands for HOMO and L denotes LUMO (E). Simplification of the charge transfer through the bridge (F).

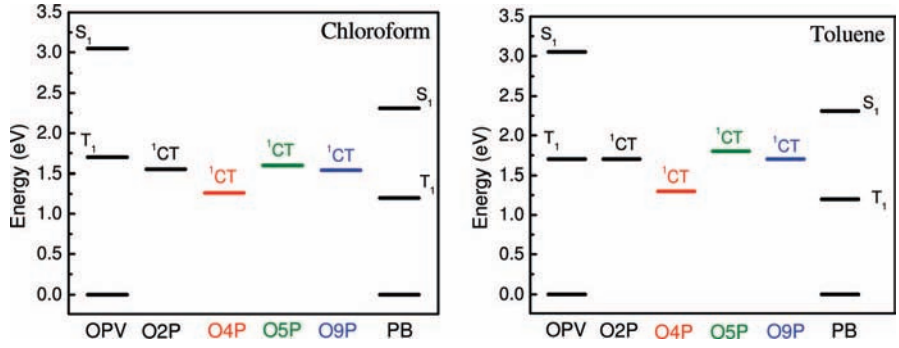

Figure 7. Energy-level diagrams for the chromophores and the corresponding charge-separated states in the foldamers (the equation for the Gibbs energy of photoinduced electron transfer was used to calculate the energy levels of the charge separated states[25]) in chloroform (left) and toluene (right).

distance through the bridge is used to ascertain the attenuation factor (Figure 5B).

The charge recombination rate decreases with increasing distance between the chromophores in the series **O4P**, **O9P**, and **O5P** in both chloroform and toluene, while **O2P** deviates which is most likely caused by the enhanced electronic interaction between the donor and acceptor through the bridge. Similar to the charge separation rate, charge recombination in **O4P** and **O2P** is faster in the more polar solvent. This behavior is characteristic of the Marcus inverted region for charge recombination[35] which is normally observed for these chromophores when recombination occurs to their ground state.[16] In contrast to the shorter oligomers, **O9P** and **O5P** in chloroform show a slower charge recombination reaction than in toluene which contradicts the expected behavior for a recombination reaction in the Marcus inverted region. This suggests that the molecules do not recombine directly to the ground state but that recombination proceeds via an intermediate higher-lying energy state, for instance a triplet state. From Figure 7 it becomes clear that the energy levels of the singlet charge separated state in toluene are somewhat higher than in chloroform. The difference in energies of the singlet charge-separated state for the different foldamers, as shown in Figure 7, follows from the different distances between the centers of the radical cations and anions in the charge separated state. The energies of the different triplet levels were obtained from previous studies.[37] Since the energies of the charge-separated states are all higher in energy than the PB triplet, charge recombination may result in the formation of PB triplets.

To probe whether charge recombination into triplet excited states occurs, near steady-state photoinduced absorption spec-

(37) (a) Ford, W. E.; Kamat, P. V. *J. Phys. Chem.* **1987**, *91*, 6373–6380. (b) van Hal, P. A.; Beckers, E. H. A.; Peeters, E.; Apperloo, J. J.; Janssen, R. A. J. *Chem. Phys. Lett.* **2000**, *328*, 403–408.

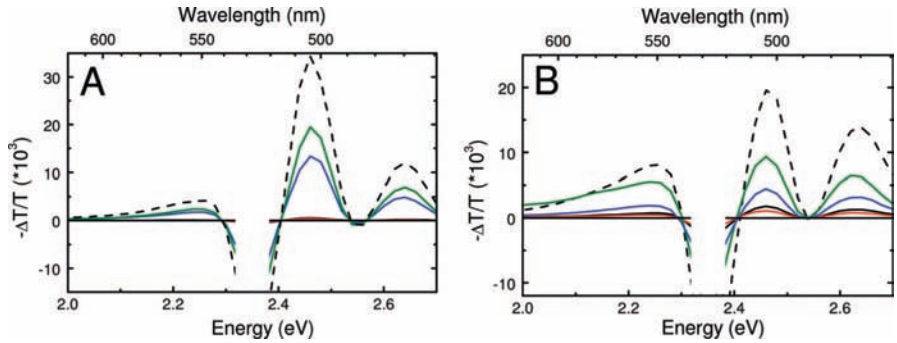

Figure 8. Near steady-state photoinduced absorption of **O2P** (black), **O4P** (red), **O5P** (green), and **O9P** (blue) in chloroform (A) and toluene (B) (λ_{exc} = 528 nm). The laser line is masked for clarity. The dashed curves are the results for a mixture of PCBM and the perylene bisimide reference, upon excitation of PCBM (λ_{exc} = 351 nm).

troscopy was employed to visualize the presence of the triplet state on the PB; the lowest triplet state in the system (Figure 7).

Excitation of the PB chromophore in each of the foldamers results in a spectrum (Figure 8) consisting of two small bands at λ = 504 (2.46 eV) and 470 nm (2.64 eV) that are typical for the T_1-T_n absorption of the PB.[37a] Irrespective of the solvent, the shorter oligomers, **O2P** and **O4P**, showed marginal amounts of triplet formation, while for the longer oligomers, **O5P** and **O9P** higher triplet yields of at least 20% were obtained.[38] The triplet excited-state lifetime of the foldamers corresponds to that measured for the **C13-PB-P**.[25] The measurements show that, indeed, charge recombination to the triplet excited state occurs. This can explain the apparent absence of Marcus inverted region behavior for the charge recombination of **O5P** and **O9P** excited states. However, further investigation is necessary to determine why for these two systems charge recombination is faster in toluene than in chloroform. Recombination from a singlet charge-separated state to a local triplet excited state can only occur if one of the electrons inverts its spin. Two mechanisms are known to describe the formation of triplet states from singlet charge separated states; radical pair and spin−orbit intersystem crossing.[39] In radical pair intersystem crossing the spins in the singlet charge-separated state dephase and evolve into the triplet charge-separated state, followed by a charge recombination to a local triplet excited state (in this case that of the PB). In spin−orbit intersystem crossing, charge recombination from the singlet charge-separated state to the local triplet excited state occurs in one step involving a change in orbital magnetic momentum that is needed for the spin flip. We note that the energy of the charge-separated state of **O4P** is the lowest of all. Since the radical cation and radical anion in **O4P** are close in space, it can be expected that the exchange energy in **O4P** is larger than for the other oligomers and places the energy of the triplet charge-separated state below the triplet energy of PB. This would inhibit that the radical pair mechanism produces the PB triplet state as observed experimentally in chloroform and to lesser extent in toluene. However, at this point we are unable to distinguish between the radical pair and spin−orbit intersystem crossing mechanism. Additional time-resolved electron spin resonance measurements might be able to clarify the mechanism that is responsible for the formation of the PB triplet.

Conclusion

We successfully attached electron-donating (OPV) and electron-accepting (PB) chromophores on rigid helical scaffolds allowing photoinduced charge transfer to occur either through space or through bridge. Molecular orbital calculations revealed significant electronic interactions through the bridging foldamer. With a variety of optical techniques we showed that excitation of the PB leads to the formation of a charge-separated state and that formation of triplet states can significantly contribute in the recombination pathway. All rates for charge separation were high and resulted in a surprisingly low attenuation factor, which is far below the value generally found for π-conjugated bridges. Attenuation factors were obtained by assuming charge separation through space or through the bridge, but each time one different foldamer needed to be discarded because it did not correlate with the behavior of the three others. Therefore, a uniform description by the current theory does not hold when a helical foldameric biomimetic bridge is used as a scaffold to organize the chromophores. Whereas in Förster energy transfer theory[40] the angle between the transition dipole moments of the photoactive units is explicitly taken into account, a similar orientation factor is less straightforward in electron-transfer theory.[41] The attenuation factor currently describes only the influence on the electronic coupling of the intervening medium at varying distance but at constant orientation. Such insights are relevant for the investigation of charge-transfer processes in both synthetic and biologic donor−bridge−acceptor systems.

Acknowledgment. The authors from Eindhoven thank NWO (Nederlandse Organisatie voor Wetenschappelijk Onderzoek) and EURYI for financial support. The authors from Amsterdam are grateful to NWO for financial support for the grant for the femtosecond equipment and to the UvA (Universiteit van Amsterdam) for structural support. Financial support from the French Ministry of Research (predoctoral fellowship to N.D.) and COST

(38) During the experiments evidence emerged that the chemical stability of the compounds were limited as a result of the triplet formation. This hampered the exact determination of the triplet quantum yields.

(39) Ahrens, M. J.; Kelley, R. F.; Dance, Z. E. X.; Wasielewski, M. R. *Phys. Chem. Chem. Phys.* **2007**, *9*, 1469–1478.

(40) Förster, T. *Ann. Phys.* **1948**, 55–75. (a) *Principles of Fluorescence Spectroscopy*; Lakowicz, J. R., Ed.; Springer: New York, 2006.

(41) Specific studies on orientation effects have been reported, see, e.g.: (a) Shin, Y.-G. K.; Newton, M. D.; Isied, S. S. *J. Am. Chem. Soc.* **2003**, *125*, 3722–3732. (b) de Gee, A. J.; Verhoeven, J. W.; Sep, W. J.; de Boer, T. J. *J. Chem. Soc. Perkin II* **1975**, 579–583. (c) Oevering, H.; Padden-Row, M. N.; Heppener, M.; Oliver, A. M.; Cotsaris, E.; Verhoeven, J. W.; Hush, N. S. *J. Am. Chem. Soc.* **1987**, *109*, 3258–3269.

action D31 (STSM of N.D.) is gratefully acknowledged. Inspiring discussions with Prof. Dr. E. W. Meijer and Dr. D. M. Bassani have been highly appreciated. We thank Dr. Xianwen Lou for the MALDI-TOF measurements and the Vietnamese Oversea Scholarship Program (VOSP) of the Vietnamese government for the support for Nguyễn Vân Anh within the UvA-HUT project.

Supporting Information Available: General methods, synthetic procedures, and characterization of **O2P**, **O4P**, **O5P**, and **O9P**, reference compound **Tetramer** and their synthetic intermediates; GPC chromatograms of the pure final compounds (Figure S1); concentration-dependent UV/vis spectroscopy in chloroform (Figure S2) and their tabulated extinction coefficients for each region in chloroform and toluene (Table S1); PL spectra in chloroform and toluene of **O2P**, **O4P**, **O5P**, **O9P** and **C13-PB-P** (Figure S3); excitation spectra in both solvents (Figure S4); femtosecond photoinduced absorption spectra in chloroform (Figure S5) and toluene (Figure S6); specification of the fitting equation for the time traces of the femtosecond photoinduced absorption measurements and their corresponding fits to the data in chloroform (Figure S7) and toluene (Figure S8); femtosecond photoinduced absorption spectra of **C13-PB-P** (Figure S9); rate constants of charge separation and charge recombination with respect to R_{DA} (Figure S10); fits to obtain the attenuation factors for charge separation and charge recombination (Figure S11); the edge-to-edge distance for each foldamer and the fit to obtain the attenuation factor while using the edge-to-edge distance (Figure S12); frequency dependence of the steady-state photoinduced absorption measurements (Figure S13); visualization of the molecular orbitals, HOMO, LUMO, and HOMO$-x$ as obtained by the calculations (Figure S14); calculated Gibbs free energy of charge separation and recombination in chloroform (Table S2) and toluene (Table S3) and the specification of the parameters used to calculate the Gibbs free energy as described by Weller. Table S4 lists the calculated values of the R_{edge}, R_{DA}, R_{Bridge}, dihedral angle α and twist angle ϕ. The cyclic voltammogram data are given in Figure S15. This material is available free of charge via the Internet at http://pubs.acs.org.

JA809367U